www.czasopisma.pan.pl PAN POLSKA AKADEMIA NAUK www.journals.pan.pl

10.1515/acsc-2016-0013

Archives of Control Sciences
Volume 26(LXII), 2016
No. 2*, pages 223–244*

Determinig of an object orientation in 3D space using direction cosine matrix and non-stationary Kalman filter

ROBERT BIEDA and KRZYSZTOF JASKOT

This paper describes a method which determines the parameters of an object orientation in 3D space. The rotation angles calculation bases on the signals fusion obtained from the inertial measurement unit (IMU). The IMU measuring system provides information from a linear acceleration sensors (accelerometers), the Earth's magnetic field sensors (magnetometers) and the angular velocity sensors (gyroscopes). Information about the object orientation is presented in the form of direction cosine matrix whose elements are observed in the state vector of the non-stationary Kalman filter. The vector components allow to determine the rotation angles (roll, pitch and yaw) associated with the object. The resulting waveforms, for different rotation angles, have no negative attributes associated with the construction and operation of the IMU measuring system. The described solution enables simple, fast and effective implementation of the proposed method in the IMU measuring systems.

Key words: direction cosine matrix, strapdown integration, IMU signals fusion, object orientation.

1. Introduction

The problem of determining the orientation of an object in space addresses a lot of aspects in many areas of life and learning. Object orientation is a very important element of the overall control of autonomous unmanned vehicles (UAVs) [1, 2, 3, 4, 5, 6]. This problem also appears in the robotics area as e.g. a definition of effector orientation of industrial manipulator, or the determination of the orientation parameters of all kinematic chains [7]. Determination of orientation is also significantly important in many implementation of medical diagnosis support to enable efficient and objective measurement of the parameters of disease with various motor dysfunctions of the human body [8, 9, 10].

This paper presents an idea of determining of an object orientation using inertial measurement unit (IMU), built in microelectromechanical systems technology (MEMS),

---

The authors are Institute of Automatic Control, Silesian University of Technology, Akademicka 16 Street, 44-100 Gliwice, Poland. Corresponding author is R. Bieda, e-mail: `robert.bieda@polsl.pl`, tel.: +48-32-237-2750, fax: +48-32-237-1165.

Received 01.12.2015. Revised 04.05.2016.

equipped with three triaxial measurement systems. To determine the parameters of rotation, defined as the angles of roll, pitch and yaw, Kalman filter algorithm is used. This algorithm pursues fusion signals available from the IMU measurement system. The proposed solution bases on a linear non-stationary process model in which the observed state is direction cosine matrix (DCM) [2, 3, 11]. This matrix defines direct object orientation (IMU measurement system) relatively to the reference system. Analysis of the individual components of the state vector makes it possible to restore the information to change the rotation angles of the object with respect to the axes of the reference frame.

2. IMU measuring system

In this study IMU system (Fig. 1) records the signal from three triaxial sensors. This sensors measure (in the system associated with a moving object) acceleration of the object (accelerometer), the Earth's magnetic field vector (magnetometer) and the changes in time of the rotation angle around each axis (gyroscopes).

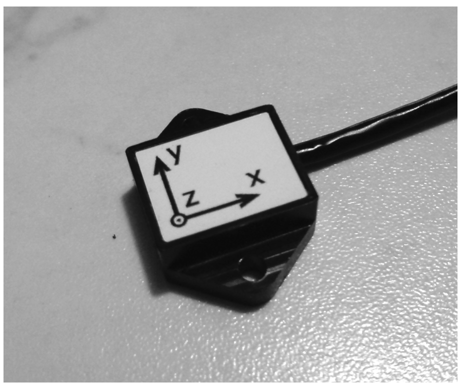

Figure 1. IMU used in the tests of the proposed algorithm for the orientation determining.

The Earth often stands for a stationary reference frame which defines the space navigation system [2, 3, 6, 11]. Typical reference are frames XYZ in different ways related to the Earth, such as ECI (Earth-Centered Inertial), ECEF (Earth-Centered, Earth-Fixed), LTP (Local Tangent Plane) including: ENU (East-North-Up) and NED (North-East-Down) [4, 3, 12]. In the presented approach, due to the intuitive definition and design of the IMU (Fig. 1), the reference frame defines the orientation of the X-axis directed to magnetic north and the Z-axis directed vertically upward from the surface of the Earth. The base frame is therefore defined in the configuration NWU (North-West-Up) as Fig. 2 shows. The changing orientation of the moving system space is defined as a coordinate frame of measuring element associated with the IMU. The coordinate frame determining the object orientation in the navigation problems is often defined as the structure of the RPY (Roll-Pitch-Yaw) [2, 3, 12], where the rotation of the axes X-Y-Z is defined appropriately as changing the angle of rotation (roll), tilt (pitch) and turning (yaw) [4, 11].

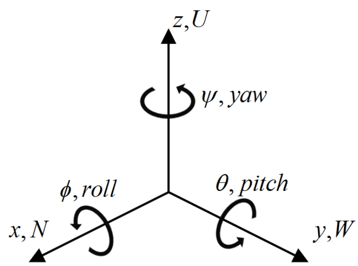

Figure 2. Definition of the NWU reference coordinate frame and angles $\phi - \theta - \psi$ which define the object's rotation.

The resulting change of orientation around each axis of the reference frame can be defined by the elementary rotation matrix around the X-Y-Z axes, respectively [4, 7, 9]:

$$
\begin{aligned}
\boldsymbol{R}_X(\phi) &= \begin{bmatrix} 1 & 0 & 0 \\ 0 & \cos(\phi) & -\sin(\phi) \\ 0 & \sin(\phi) & \cos(\phi) \end{bmatrix} \\
\boldsymbol{R}_Y(\theta) &= \begin{bmatrix} \cos(\theta) & 0 & \sin(\theta) \\ 0 & 1 & 0 \\ -\sin(\theta) & 0 & \cos(\theta) \end{bmatrix} \\
\boldsymbol{R}_Z(\psi) &= \begin{bmatrix} \cos(\psi) & -\sin(\psi) & 0 \\ \sin(\psi) & \cos(\psi) & 0 \\ 0 & 0 & 1 \end{bmatrix}
\end{aligned}
\tag{1}
$$

where ϕ, θ, ψ define the value of the rotation angle around the X-axis (roll), the Y-axis (pitch) and Z-axis (yaw) of the RPY frame associated with the measuring IMU device, expressed relatively to the NWU reference frame.

3. Rotation matrix

The transformation $\boldsymbol{R} \in SO(3)$ (Special Orthogonal group) [7, 13, 14, 15] defines an orthogonal rotation tensor operator in three-dimensional space and has the following characteristics:

$$\boldsymbol{R}^{-1} = \boldsymbol{R}^T, \ \ \boldsymbol{R}\boldsymbol{R}^T = \boldsymbol{R}^T\boldsymbol{R} = \boldsymbol{I}^{3\times 3}, \ \ \det(\boldsymbol{R}) = \pm 1. \tag{2}$$

The case $\det(\boldsymbol{R}) = -1$ occurs when one of the base (space) forms a right-handed coordinate frame and the second base forms a left-handed coordinate frame [13]. Such a case is not considered in this paper because we discuss the situation where the second base is formed by the rotation of the first base. The transformation matrix $\boldsymbol{R}$ therefore determines the rotation transformation of the one three-dimensional space relative to the other. In the inertial navigation, especially in aviation, the homogeneous transformation matrix corresponding to the rotation of the $\psi - \theta - \phi$ angles [6, 16] (by $\phi - \theta - \psi$ angles relative to the original/base NWU reference frame) can be defined by an elementary rotation matrix around each axis (1). Rotation matrix defining the transformation of the transition from the basic (fixed) NWU frame subject to the rotation RPY frame is defined as follows [1, 4, 9, 11]:

$$\boldsymbol{R}_{RPY}^{NWU} = \boldsymbol{R}_Z(\psi)\boldsymbol{R}_Y(\theta)\boldsymbol{R}_X(\phi) = \begin{bmatrix} c_\theta c_\psi & s_\phi s_\theta c_\psi - c_\phi s_\psi & c_\phi s_\theta c_\psi + s_\phi s_\psi \\ c_\theta s_\psi & s_\phi s_\theta s_\psi + c_\phi c_\psi & c_\phi s_\theta s_\psi - s_\phi c_\psi \\ -s_\theta & s_\phi c_\theta & c_\phi c_\theta \end{bmatrix} \tag{3}$$

where $c_\alpha = \cos(\alpha), s_\alpha = \sin(\alpha)$.

Rotation matrix (3) allows to specify the orientation of the object in the base NWU frame using knowledge of the $\phi - \theta - \psi$ angles and information about the object expressed in the IMU measurement frame. However, the inverse rotation transformation in XYZ Euler angles ($\phi - \theta - \psi$) notation, can be defined as a rotation in the opposite (inverse) direction around the axis ZYX of the primary (rotating) RPY frame associated with the IMU measurement frame:

$$\begin{aligned}\boldsymbol{R}_{NWU}^{RPY} &= \boldsymbol{R}_X(-\phi)\boldsymbol{R}_Y(-\theta)\boldsymbol{R}_Z(-\psi) = \boldsymbol{R}_X(\phi)^{-1}\boldsymbol{R}_Y(\theta)^{-1}\boldsymbol{R}_Z(\psi)^{-1} = \\ &= \boldsymbol{R}_X(\phi)^T\boldsymbol{R}_Y(\theta)^T\boldsymbol{R}_Z(\psi)^T = \begin{bmatrix} c_\theta c_\psi & c_\theta s_\psi & -s_\theta \\ s_\phi s_\theta c_\psi - c_\phi s_\psi & s_\phi s_\theta s_\psi + c_\phi c_\psi & s_\phi c_\theta \\ c_\phi s_\theta c_\psi + s_\phi s_\psi & c_\phi s_\theta s_\psi - s_\phi c_\psi & c_\phi c_\theta \end{bmatrix}\end{aligned} \tag{4}$$

where $c_\alpha = \cos(\alpha), s_\alpha = \sin(\alpha)$.

The transformations (3) and (4) have the properties of rotation operators $\boldsymbol{R} \in SO(3)$, and are often referred as the DCM [2, 3, 11]. Transformations (3), (4) and DCM are associated with each other according to the following relationship:

$$\begin{aligned}\boldsymbol{R}_{RPY}^{NWU} &= \begin{bmatrix} \mathbf{1}_R & \mathbf{1}_P & \mathbf{1}_Y \end{bmatrix} = \begin{bmatrix} c_{NR} & c_{NP} & c_{NY} \\ c_{WR} & c_{WP} & c_{WY} \\ c_{UR} & c_{UP} & c_{UY} \end{bmatrix} = \begin{bmatrix} \mathbf{1}_N^T \\ \mathbf{1}_W^T \\ \mathbf{1}_U^T \end{bmatrix} \\ &= \begin{bmatrix} \mathbf{1}_N & \mathbf{1}_W & \mathbf{1}_U \end{bmatrix}^T = \left(\boldsymbol{R}_{NWU}^{RPY}\right)^{-1}\end{aligned} \tag{5}$$

where $\mathbf{1}_i$ is the i-th unit vector of the axis of the space frame, while the DCM matrix coefficient $c_{ij} = \mathbf{1}_i^T \mathbf{1}_j = \cos(\beta)$ determines cosine of the angle between the i-th axis NWU base frame and the j-th axis RPY measuring frame.

4. Calculation of RPY object orientation

The IMU measurement system is constructed using the MEMS technology [1, 3, 17]. This system is equipped with three triaxial measurement systems defined in the configuration of the reference frame associated with the fixed NWU coordinate frame of the Earth.

4.1. Accelerometers

Model of the acceleration signal measured by the accelerometers system is defined as the sum of the actual value of acceleration $\widetilde{\boldsymbol{a}}$, gravity vector $\boldsymbol{g}$ and component $\boldsymbol{v}_a$ modeling Gaussian white noise [8, 10]:

$$\boldsymbol{a} = \widetilde{\boldsymbol{a}} - \boldsymbol{g} + \boldsymbol{v}_a \tag{6}$$

Analyzing the ideal case (without noise), triaxial accelerometer system measures the acceleration $\boldsymbol{a}^A = \begin{bmatrix} a_x & a_y & a_z \end{bmatrix}^T$ as the projection of acceleration vector on the axes of measurement frame in the RPY space [14, 16]:

$$\boldsymbol{a}^A = \begin{bmatrix} a_x \\ a_y \\ a_z \end{bmatrix} = \boldsymbol{R}_{NWU}^{RPY} \left(\widetilde{\boldsymbol{a}} - \boldsymbol{g} \right) \tag{7}$$

where $\widetilde{\boldsymbol{a}}$ and $\boldsymbol{g} = \begin{bmatrix} 0 & 0 & -g \end{bmatrix}^T$ are: object acceleration vector and vector acceleration of gravity $\left(g \approx 9.81 \left[m/s^2 \right] \right)$, respectively (see Fig. 3) expressed in the NWU reference frame.

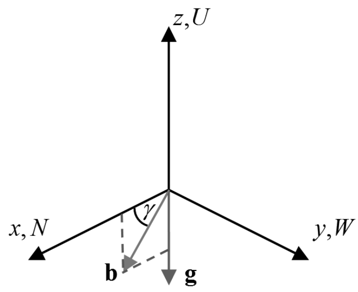

Figure 3. Position of the acceleration of gravity vector $\boldsymbol{g}$ and the Earth's magnetic field vector $\boldsymbol{b}$ in the NWU reference frame.

We assume that the value of acceleration associated with the object is negligibly small ($\widetilde{\boldsymbol{a}} \approx \mathbf{0}$) [18].

Assuming that the value of the acceleration associated with the object movement is negligibly small one may approximately assume that the accelerometer system measures projection of the constant acceleration of gravity vector expressed in the IMU measurement coordinate frame. Using the rotation operator $\boldsymbol{R}_{NWU}^{RPY}$ the acceleration of gravity vector $\boldsymbol{g}$ can be expressed in the RPY frame:

$$-\boldsymbol{g}^{RPY} = \boldsymbol{R}_{NWU}^{RPY}(-\boldsymbol{g}) = \begin{bmatrix} -s_\theta g \\ s_\phi c_\theta g \\ c_\phi c_\theta g \end{bmatrix} \approx \begin{bmatrix} a_x \\ a_y \\ a_z \end{bmatrix} = \boldsymbol{a}^A. \tag{8}$$

Using equation (8), and the result of measurement $\boldsymbol{a}^A$ from linear acceleration sensors [18, 19] the values of the angles of object rotation roll (ϕ) (9) and pitch (θ) (10) can be determined as follows:

$$\left.\begin{array}{r} s_\phi c_\theta g = a_y \\ c_\phi c_\theta g = a_z \end{array}\right\} \Rightarrow \tan(\phi) = \frac{a_y}{a_z} \Rightarrow \phi = \arctan\left(\frac{a_y}{a_z}\right) \tag{9}$$

$$-s_\theta g = a_x \Rightarrow \sin(\theta) = \frac{a_x}{-g} \Rightarrow \theta = \arcsin\left(\frac{-a_x}{g}\right) \tag{10}$$

or using the property $\sqrt{a_y^2 + a_z^2} = c_\theta g$:

$$\left.\begin{array}{r} -s_\theta g = a_x \\ \sqrt{a_y^2 + a_z^2} = c_\theta g \end{array}\right\} \Rightarrow \tan(\theta) = \frac{-a_x}{\sqrt{a_y^2 + a_z^2}} \Rightarrow \theta = \arctan\left(\frac{-a_x}{\sqrt{a_y^2 + a_z^2}}\right). \tag{11}$$

To ensure the distinguishability of the results of the calculation of the angle, one should use the arctan2 (two-arguments arctangent) which returns an angle in the range $\pm\pi$:

$$\phi = \arctan\left(\frac{a_y}{a_z}\right) \Rightarrow \{\phi \sim \pm\pi\} \Rightarrow \phi = \arctan2(a_y, a_z). \tag{12}$$

Analysis based on the values returned by the accelerometer system cannot determine all three rotation angles of RPY. In order to determine the angle yaw, using of the magnetic compass system implemented by the three-axis magnetometer is required.

4.2. Magnetometers

The signal measured by the magnetometer system is modeled as the sum of the Earth's magnetic field vector $\widetilde{\boldsymbol{b}}$ and $\boldsymbol{v}_m$ modeling white noise measurement [8]:

$$\boldsymbol{m} = \widetilde{\boldsymbol{b}} + \boldsymbol{v}_m. \tag{13}$$

The triaxial magnetometer system used in the IMU, measures the projection of the Earth's magnetic field vector $\widetilde{\boldsymbol{b}} = \begin{bmatrix} B\cos(\gamma) & 0 & -B\sin(\gamma) \end{bmatrix}^T$ in the object RPY coordinate frame. The angle γ defines the inclination of the magnetic field vector of the reference frame on XY plane. The value of this angle varies depending on the latitude from $0\,[deg]$ on the equator to $\pm 90\,[deg]$ on the magnetic poles. Similarly, the magnetic field strength B is dependent on the latitude. In order to make scaling process independent on the magnetometer measuring on the intensity of the Earth's magnetic field, the value of the intensity magnetic field vector is normalized ($\|\boldsymbol{b}\| = \left\|\frac{\tilde{\boldsymbol{b}}}{B}\right\| = 1$) [10]. Construction of the IMU magnetometer sensor is compatible with the configuration of the base NWU coordinate frame of the Earth (Fig. 3). Therefore, the triaxial magnetometer measures projections $\boldsymbol{m}^M = \begin{bmatrix} m_x & m_y & m_z \end{bmatrix}^T$ of normalized magnetic field vector $\boldsymbol{b} = \begin{bmatrix} \cos(\gamma) & 0 & -\sin(\gamma) \end{bmatrix}^T$ [16] in the RPY frame [8, 14]:

$$\boldsymbol{m}^M = \boldsymbol{R}_{NWU}^{RPY}\boldsymbol{b} = \boldsymbol{R}_X(\phi)^T \boldsymbol{R}_Y(\theta)^T \boldsymbol{R}_Z(\psi)^T \boldsymbol{b}. \tag{14}$$

Transforming the above relation, we obtain [20]:

$$\begin{gathered} \boldsymbol{R}_Y(\theta)\,\boldsymbol{R}_X(\phi)\,\boldsymbol{m}^M = \boldsymbol{R}_Z(\psi)^T\boldsymbol{b} = \boldsymbol{b}^r = \\ = \begin{bmatrix} c_\theta m_x + s_\phi s_\theta m_y + c_\phi s_\theta m_z \\ c_\phi m_y - s_\phi m_z \\ -s_\theta m_x + s_\phi c_\theta m_y + c_\phi c_\theta m_z \end{bmatrix} = \begin{bmatrix} c_\theta c_\gamma \\ -s_\theta c_\gamma \\ -s_\gamma \end{bmatrix} = \begin{bmatrix} b_x^r \\ b_y^r \\ b_z^r \end{bmatrix}. \end{gathered} \tag{15}$$

From the comparison of corresponding output vector elements [19] we obtain the dependence on the value of the yaw angle (ψ) [20]:

$$\begin{gathered} \left.\begin{array}{r} c_\theta c_\gamma = b_x^r \\ -s_\theta c_\gamma = b_y^r \end{array}\right\} \Rightarrow \tan(\psi) = \frac{-b_y^r}{b_x^r} = \frac{-\left(c_\phi m_y - s_\phi m_z\right)}{c_\theta m_x + s_\phi s_\theta m_y + c_\phi s_\theta m_z} \\ \Rightarrow \psi = \arctan\left(\frac{s_\phi m_z - c_\phi m_y}{c_\theta m_x + s_\phi s_\theta m_y + c_\phi s_\theta m_z}\right). \end{gathered} \tag{16}$$

Similarly to the case of determining the value of the roll angle (12) in determining the value of the yaw angle we use two-arguments arctangent:

$$\begin{gathered} \psi = \arctan\left(\frac{s_\phi m_z - c_\phi m_y}{c_\theta m_x + s_\phi s_\theta m_y + c_\phi s_\theta m_z}\right) \Rightarrow \{\psi \sim \pm\pi\} \\ \Rightarrow \psi = \operatorname{arctan2}\left(\left(s_\phi m_z - c_\phi m_y\right), \left(c_\theta m_x + s_\phi s_\theta m_y + c_\phi s_\theta m_z\right)\right). \end{gathered} \tag{17}$$

Because of the noise occurring in the accelerometers (6) and magnetometers (13) measurement systems values which determine rotation angles change rapidly. It is then often low pass filtering applied while determining roll, pitch and yaw angles. It aims at eliminating noise in the designated values of the angles resulting from the noise presented in the signals measured in the IMU system. The angles of rotation defined by the strapdown integration of the signal from the gyroscopes do not cause such a problem.

4.3. Gyroscopes

The third system of sensors used in the IMU is triaxial gyroscope. The signal measured by the gyroscopes system is modeled by the sum of angular velocity vector $\tilde{\boldsymbol{\omega}}$, bias vector $\boldsymbol{\beta}$ and white noise $\boldsymbol{v}_\omega$ [8, 16]:

$$\boldsymbol{\omega} = \tilde{\boldsymbol{\omega}} + \boldsymbol{\beta} + \boldsymbol{v}_\omega. \tag{18}$$

In the ideal case (without bias and distortion) gyroscopes return information about the variation of the rotation angle around the axis of the rotating RPY frame. As the result, the signal from the gyroscopes can be defined as the angular velocity vector $\boldsymbol{\omega}^G = \begin{bmatrix} \omega_x & \omega_y & \omega_z \end{bmatrix}^T$ for each axis of the IMU measurement system. Using information about the homogeneous transformation matrix $\boldsymbol{R}_{RPY}^{NWU}$ (3):

$$\boldsymbol{R}_{RPY}^{NWU} = \begin{bmatrix} c_\theta c_\psi & s_\phi s_\theta c_\psi - c_\phi s_\psi & c_\phi s_\theta c_\psi + s_\phi s_\psi \\ c_\theta s_\psi & s_\phi s_\theta s_\psi + c_\phi c_\psi & c_\phi s_\theta s_\psi - s_\phi c_\psi \\ -s_\theta & s_\phi c_\theta & c_\phi c_\theta \end{bmatrix} = \begin{bmatrix} r_{11} & r_{12} & r_{13} \\ r_{21} & r_{22} & r_{23} \\ r_{31} & r_{32} & r_{33} \end{bmatrix} \tag{19}$$

the object rotation angles roll, pitch and yaw can be determined from a comparison of the respective elements $(row, column)$ of the matrix (19) [1]. The comparison of elements $(3,2)$ and $(3,3)$ gives the angle of roll:

$$\left.\begin{aligned} s_\phi c_\theta &= r_{32} \\ c_\phi c_\theta &= r_{33} \end{aligned}\right\} \Rightarrow \tan(\phi) = \frac{r_{32}}{r_{33}} \Rightarrow \phi = \arctan\left(\frac{r_{32}}{r_{33}}\right). \tag{20}$$

Comparison of element $(3,1)$ can be determined by the pitch angle:

$$-s_\theta = r_{31} \Rightarrow \sin(\theta) = -r_{31} \Rightarrow \theta = \arcsin(-r_{31}) \tag{21}$$

or using the property $\sqrt{r_{32}^2 + r_{33}^2} = c_\theta$:

$$\left.\begin{aligned} -s_\theta &= r_{31} \\ \sqrt{r_{32}^2 + r_{33}^2} &= c_\theta \end{aligned}\right\} \Rightarrow \tan(\theta) = \frac{-r_{31}}{\sqrt{r_{32}^2 + r_{33}^2}} \Rightarrow \theta = \arctan\left(\frac{-r_{31}}{\sqrt{r_{32}^2 + r_{33}^2}}\right). \tag{22}$$

The yaw angle value is obtained from the comparison of components $(1,1)$ and $(2,1)$:

$$\left.\begin{aligned} c_\theta s_\psi &= r_{21} \\ c_\theta c_\psi &= r_{11} \end{aligned}\right\} \Rightarrow \tan(\psi) = \frac{r_{21}}{r_{11}} \Rightarrow \psi = \arctan\left(\frac{r_{21}}{r_{11}}\right). \tag{23}$$

Similarly to results obtained from the accelerometers and the magnetometers, the range of variation angle provides uniqueness of the solution [4]. To determine the angles ϕ and ψ we have used the $\arctan2(Y,X)$ function which returns the angle in the range $\pm\pi$:

$$\phi = \arctan\left(\frac{r_{32}}{r_{33}}\right) \Rightarrow \{\phi \sim \pm\pi\} \Rightarrow \phi = \arctan2(r_{32}, r_{33}) \tag{24}$$

$$\psi = \arctan\left(\frac{r_{21}}{r_{11}}\right) \Rightarrow \{\psi \sim \pm\pi\} \Rightarrow \psi = \text{arctan2}\left(r_{21}, r_{11}\right). \tag{25}$$

5. The equation of rotation motion

The equations (20), (22) and (23) describe angles which can be determined using the rotation matrix $\boldsymbol{R}_{RPY}^{NWU}$ (3). The angular velocity vector $\boldsymbol{\omega}^G$ can be treated as a pseudo-rotation vector [2]. The IMU system (RPY coordinate frame) is rotated around this pseudo-rotation vector as Fig. 4) shows.

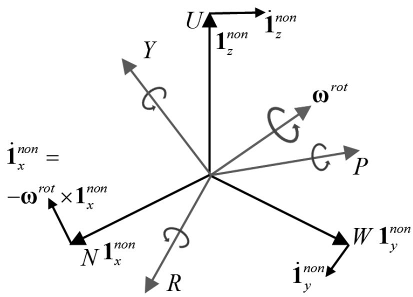

Figure 4. Seeming rotation of the NWU reference frame in response to rotation of the RPY measuring frame around the pseudo-rotation vector $\boldsymbol{\omega}^{rot}$.

Rotation of the RPY frame associated with the object (rotating frame - *rot*) seen in the IMU system generates a seeming rotation of the NWU reference frame associated with the Earth (non-rotating frame - *non*) in the direction opposite to the direction defined by the pseudo-rotation vector $\boldsymbol{\omega}^{rot}$. Denote by $\boldsymbol{C}_{non}^{rot}$ direction cosine matrix (rotation matrix) defining the transformation of the moving (*rot*) frame to the stationary (*non*) frame to determine the relationship of the rotation matrix (4):

$$\boldsymbol{R}_{NWU}^{RPY} = \begin{bmatrix} \mathbf{1}_N & \mathbf{1}_W & \mathbf{1}_U \end{bmatrix} = \boldsymbol{C}_{non}^{rot} = \begin{bmatrix} \mathbf{1}_x^{non} & \mathbf{1}_y^{non} & \mathbf{1}_z^{non} \end{bmatrix}. \tag{26}$$

Using pseudo-rotation vector $\boldsymbol{\omega}^{rot}$ and right-hand rule, it can be shown that the linear velocity versors of axis stationary frame (NWU), caused by seeming rotation of this frame are set by the formula [2]:

$$\begin{cases} \frac{d}{dt}\mathbf{1}_x^{non} = -\boldsymbol{\omega}^{rot} \times \mathbf{1}_x^{non} \\ \frac{d}{dt}\mathbf{1}_y^{non} = -\boldsymbol{\omega}^{rot} \times \mathbf{1}_y^{non} \\ \frac{d}{dt}\mathbf{1}_z^{non} = -\boldsymbol{\omega}^{rot} \times \mathbf{1}_z^{non}. \end{cases} \tag{27}$$

Using (26) it can be shown that the change in time, the rotation operator $\boldsymbol{C}_{non}^{rot}$ is determined by the relation:

$$\frac{d}{dt}\boldsymbol{C}_{non}^{rot} = \begin{bmatrix} \frac{d}{dt}\mathbf{1}_x^{non} & \frac{d}{dt}\mathbf{1}_y^{non} & \frac{d}{dt}\mathbf{1}_z^{non} \end{bmatrix}. \tag{28}$$

Using the equations of linear velocities (27) it can be shown the following relationship between the rotation of pseudo-rotation vector $\boldsymbol{\omega}^{rot}$ [13] and the change in the rotation matrix (28):

$$\begin{aligned} \frac{d}{dt}\boldsymbol{C}_{non}^{rot} &= \begin{bmatrix} -\boldsymbol{\omega}^{rot} \times \mathbf{1}_x^{non} & -\boldsymbol{\omega}^{rot} \times \mathbf{1}_y^{non} & -\boldsymbol{\omega}^{rot} \times \mathbf{1}_z^{non} \end{bmatrix} = \\ &= -\boldsymbol{\omega}^{rot} \times \begin{bmatrix} \mathbf{1}_x^{non} & \mathbf{1}_y^{non} & \mathbf{1}_z^{non} \end{bmatrix} = -\left[\boldsymbol{\omega}^{rot}\times\right]\boldsymbol{C}_{non}^{rot} \end{aligned} \tag{29}$$

where $[\boldsymbol{\omega}^{rot}\times]$ is skew-symmetric matrix [13] (the cross-product operator). Assuming that the pseudo-rotation vector is equal to the vector angular velocities measured by the gyroscopes system: $\boldsymbol{\omega}^{rot} = \begin{bmatrix} \omega_x & \omega_y & \omega_z \end{bmatrix}^T = \boldsymbol{\omega}^G$, the skew-symmetric tensor with axial vector $\boldsymbol{\omega}^{rot}$ [13] is defined as follows [1, 2, 3, 21, 15]:

$$\left[\boldsymbol{\omega}^{rot}\times\right] = \begin{bmatrix} 0 & -\omega_z & \omega_y \\ \omega_z & 0 & -\omega_x \\ -\omega_y & \omega_x & 0 \end{bmatrix}. \tag{30}$$

The equations defining the angles roll (24), pitch (21, 22) and yaw (25) use information about the elements of the transformation matrix $\boldsymbol{R}_{RPY}^{NWU}$ of the reference NWU frame (non-rotating frame - *non*) to the RPY frame (rotating frame - *rot*) associated with the movable object. We can denote this as a DCM transformation $\boldsymbol{C}_{rot}^{non}$:

$$\boldsymbol{R}_{RPY}^{NWU} = \begin{bmatrix} \mathbf{1}_R & \mathbf{1}_P & \mathbf{1}_Y \end{bmatrix} = \boldsymbol{C}_{rot}^{non}. \tag{31}$$

Using the properties of orthogonal rotation tensor $\boldsymbol{R}$ (2):

$$\boldsymbol{C}_{rot}^{non} = \left(\boldsymbol{C}_{non}^{rot}\right)^{-1} = \left(\boldsymbol{C}_{non}^{rot}\right)^T \tag{32}$$

and equation (29) we can determine the equation for generating the rotation of the direction cosine matrix $\boldsymbol{C}_{rot}^{non}$ [1, 2]:

$$\begin{aligned} \frac{d}{dt}\boldsymbol{C}_{rot}^{non} &= \frac{d}{dt}\left(\boldsymbol{C}_{non}^{rot}\right)^T = \left(\frac{d}{dt}\boldsymbol{C}_{non}^{rot}\right)^T = \left(-\left[\boldsymbol{\omega}^{rot}\times\right]\boldsymbol{C}_{non}^{rot}\right)^T = \\ &= -\left(\boldsymbol{C}_{non}^{rot}\right)^T\left[\boldsymbol{\omega}^{rot}\times\right]^T = \boldsymbol{C}_{rot}^{non}\left[\boldsymbol{\omega}^{rot}\times\right]. \end{aligned} \tag{33}$$

Assuming, as before, that $\boldsymbol{\omega}^{rot} = \boldsymbol{\omega}^G$ and using relation (31) we can show that equation (33) takes the following form [6, 10]:

$$\frac{d}{dt}\boldsymbol{R}_{RPY}^{NWU} = \boldsymbol{R}_{RPY}^{NWU}\left[\boldsymbol{\omega}^G\times\right] \tag{34}$$

where $\left[\boldsymbol{\omega}^G \times\right]$ is skew-symmetric matrix as in (30).

In order to determine the rotation matrix $\boldsymbol{C}_{rot}^{non}$ ($\boldsymbol{R}_{RPY}^{NWU}$) one needs to solve differential equation (33, 34). One possibility is to define an approximate solution [21] based on the replacement of the derivative operation by operation of the finite difference in time period Δt [1, 11]:

$$\frac{d}{dt}\boldsymbol{C}_{rot}^{non}(t) = \dot{\boldsymbol{C}}_{rot}^{non}(t) = \lim_{dt \to 0} \frac{\boldsymbol{C}_{rot}^{non}(t+dt) - \boldsymbol{C}_{rot}^{non}(t)}{dt} \approx \frac{\boldsymbol{C}_{rot}^{non}(t+\Delta t) - \boldsymbol{C}_{rot}^{non}(t)}{\Delta t}. \tag{35}$$

Using (35) an iterative formula can be derived to determine the matrix $\boldsymbol{C}_{rot}^{non}(t)$ in successive moments of time:

$$\boldsymbol{C}_{rot}^{non}(t+\Delta t) = \boldsymbol{C}_{rot}^{non}(t) + \dot{\boldsymbol{C}}_{rot}^{non}(t)\,\Delta t \tag{36}$$

where Δt is the period between discrete moments of time (the sampling period in the IMU system).

For small rotation angles $\alpha \in \{\phi, \theta, \psi\}$ one can assume that $\sin(\alpha) \approx \alpha$ and $\cos(\alpha) \approx 1$ [21]. As the result, the rotation matrix $\boldsymbol{C}_{rot}^{non}$ ($\boldsymbol{R}_{RPY}^{NWU}$) (3) can be approximated as follows [1, 12, 11]:

$$\boldsymbol{C}_{rot}^{non}(t) \approx \begin{bmatrix} 1 & -\psi & \theta \\ \psi & 1 & -\phi \\ -\theta & \phi & 1 \end{bmatrix} \tag{37}$$

Based on the approximate form of rotation matrix (37) sequence generating rotation (33, 34) can be expressed as follows [11]:

$$\dot{\boldsymbol{C}}_{rot}^{non}(t) \approx \boldsymbol{C}_{rot}^{non}(t) \begin{bmatrix} 0 & -\dot{\psi} & \dot{\theta} \\ \dot{\psi} & 0 & -\dot{\phi} \\ -\dot{\theta} & \dot{\phi} & 0 \end{bmatrix}. \tag{38}$$

Using approximation (38), and taking into account the relationship:

$$\dot{\alpha}(t) = \frac{d\alpha(t)}{dt} = \omega(t) \approx \frac{\alpha(t+\Delta t) - \alpha(t)}{\Delta t} = \frac{\Delta\alpha(t)}{\Delta t} \tag{39}$$

the component of updating solution in equation (36) takes now the form [1]:

$$\begin{aligned} \dot{\boldsymbol{C}}_{rot}^{non}(t)\,\Delta t &\approx \boldsymbol{C}_{rot}^{non}(t) \begin{bmatrix} 0 & -\dot{\psi} & \dot{\theta} \\ \dot{\psi} & 0 & -\dot{\phi} \\ -\dot{\theta} & \dot{\phi} & 0 \end{bmatrix} \Delta t \approx \boldsymbol{C}_{rot}^{non}(t) \begin{bmatrix} 0 & -\Delta\psi & \Delta\theta \\ \Delta\psi & 0 & -\Delta\phi \\ -\Delta\theta & \Delta\phi & 0 \end{bmatrix} = \\ &= \boldsymbol{C}_{rot}^{non}(t)\left[\boldsymbol{\omega}^{rot} \times\right]\Delta t = \boldsymbol{C}_{rot}^{non}(t)\,[\boldsymbol{A}\times] \end{aligned} \tag{40}$$

where $[\boldsymbol{A}\times]$ is skew-symmetric matrix:

$$[\boldsymbol{A}\times] = \begin{bmatrix} 0 & -\omega_z\Delta t & \omega_y\Delta t \\ \omega_z\Delta t & 0 & -\omega_x\Delta t \\ -\omega_y\Delta t & \omega_x\Delta t & 0 \end{bmatrix}. \tag{41}$$

Using these relationships, and information obtained from the measurement system of gyroscopes, equation (36) which defines the rotation matrix $\boldsymbol{R}_{RPY}^{NWU}$ can be denoted in the form [8, 22]:

$$\boldsymbol{R}_{RPY}^{NWU}(t+\Delta t) = \boldsymbol{R}_{RPY}^{NWU}(t)\left(\boldsymbol{I}^{3\times3} + [\boldsymbol{A}\times]\right) = \boldsymbol{R}_{RPY}^{NWU}(t)\,\boldsymbol{\Omega} \tag{42}$$

where:

$$\boldsymbol{\Omega} = \begin{bmatrix} 1 & -\Delta\psi & \Delta\theta \\ \Delta\psi & 1 & -\Delta\phi \\ -\Delta\theta & \Delta\phi & 1 \end{bmatrix} = \boldsymbol{I}^{3\times3} + [\boldsymbol{A}\times] = \begin{bmatrix} 1 & -\omega_z\Delta t & \omega_y\Delta t \\ \omega_z\Delta t & 1 & -\omega_x\Delta t \\ -\omega_y\Delta t & \omega_x\Delta t & 1 \end{bmatrix}. \tag{43}$$

The rotation angles ϕ, θ, ψ determined from the $\boldsymbol{R}_{RPY}^{NWU}$ matrix obtained as a result of the integration process do not change so rapidly as in the case of noise $\boldsymbol{v}_\omega$ influence on the angular velocities vector $\boldsymbol{\omega}^G$ (18). In contrast to the rotation angles determined from the accelerometers and magnetometers, the angles determined from the gyroscopes are devoid of the element "nervousness" in the time course. However, the bias $\boldsymbol{\beta}$ (18) presented in the signal obtained from the gyroscopes is cumulated in the process of integration. This results in a slow but continuous change in the designated of rotation angles. The resulting phenomena is the "flow" of the values of angles. Both of the values of angles determined from the measurements of the gyroscopes and accelerometers and magnetometers systems are specific to the measurement system errors. One way of correcting the rotation angles is to design the so-called complementary filter [5, 9, 16, 22, 23, 24]. However, often the correction process is implemented as a fusion of signals containing information about the orientation of the different sources of measurement. This process is performed using the algorithm of the observer which is constituted by the Kalman filter. It allows the estimation of unmeasured signals based on the available signals and process model.

6. The signals fusion

Kalman filter [1, 2, 3] is a basic mathematical tool which allows observation of immeasurable signals using available measurements and process model. In the problem of determining the object orientation measurable quantities are the signals from the accelerometers $\boldsymbol{a}^A$ (8), magnetometers $\boldsymbol{m}^M$ (14) and gyroscopes $\boldsymbol{\omega}^G$ (18). When measuring using the IMU we are dealing with a discrete process in which measurements are available at certain period of time Δt. For this type of problems the Kalman filter system is described by a discrete model [25] equation of state changes (process equation) and output equation (measurement equation) [8, 9]:

$$\begin{aligned} \boldsymbol{x}_k &= \boldsymbol{F}\boldsymbol{x}_{k-1} + \boldsymbol{v}_k \\ \boldsymbol{y}_k &= \boldsymbol{H}\boldsymbol{x}_k + \boldsymbol{w}_k \end{aligned} \tag{44}$$

where $\boldsymbol{F}$ and $\boldsymbol{H}$ are the matrices of the model of state and output equations, $\boldsymbol{x}_k \in \Re^n$ and $\boldsymbol{y}_k \in \Re^m$ are the state vector and the output vector (measured) at $k = 1/\Delta t$, $\boldsymbol{v}_k \in \Re^n$ and $\boldsymbol{w}_k \in \Re^m$ are, respectively, the distortion and measurement noise modeled as a random value with zero expected value $E[\boldsymbol{v}] = E[\boldsymbol{w}] = \boldsymbol{0}$ and variance $\boldsymbol{V} = E\left[\boldsymbol{v}\boldsymbol{v}^T\right]$ and $\boldsymbol{W} = E\left[\boldsymbol{w}\boldsymbol{w}^T\right]$. The process of determining the state vector (observed value) can be divided into two stages:

- the prediction step, wherein the state and covariance matrix estimation is made on the basis of the process model:

$$\begin{aligned} \hat{\boldsymbol{x}}_{k|k-1} &= \boldsymbol{F}\hat{\boldsymbol{x}}_{k-1|k-1} \\ \boldsymbol{P}_{k|k-1} &= \boldsymbol{F}\boldsymbol{P}_{k-1|k-1}\boldsymbol{F}^T + \boldsymbol{V} \end{aligned} \tag{45}$$

  where $\hat{\boldsymbol{x}}_k \in \Re^n$ is the predicted estimate of the process state, and $\boldsymbol{P}$ is the covariance matrix;

- the correction stage in which the correction of the state and covariance matrix estimate bases on the measurement:

$$\begin{aligned} \boldsymbol{K}_k &= \boldsymbol{P}_{k|k-1}\boldsymbol{H}^T\left(\boldsymbol{H}\boldsymbol{P}_{k|k-1}\boldsymbol{H}^T + \boldsymbol{W}\right)^{-1}, \\ \hat{\boldsymbol{x}}_{k|k} &= \hat{\boldsymbol{x}}_{k|k-1} + \boldsymbol{K}_k\left(\boldsymbol{y}_k - \boldsymbol{H}\hat{\boldsymbol{x}}_{k|k-1}\right), \\ \boldsymbol{P}_{k|k} &= \left(\boldsymbol{I} - \boldsymbol{K}_k\boldsymbol{H}\right)\boldsymbol{P}_{k|k-1} \end{aligned} \tag{46}$$

  where $\boldsymbol{K}_k$ is the gain matrix of the Kalman filter.

Due to the properties of the measuring system, the fusion of information obtained from accelerometers and gyroscopes affected by bias is implemented. Difficulties in reconstruction of rotation angles directly from measurements of angular velocities often cause the representation of rotation operations by the quaternions description [1, 2, 3, 4, 6, 7, 9, 16, 26, 15]. Another approach to the information fusion process is the use of so-called complementary Kalman filter [8, 12, 14, 19, 23, 25, 27]. Unlike the classical approach in the complementary Kalman filter, state vector is not observed. The only observed are values of errors.

In the proposed solution, the Kalman filter was used in its classical form directly based on the state vector (observed value). In contrast to the solutions of the problem, in the proposed approach the rotation angles $\phi - \theta - \psi$ are estimated implicitly using orthogonal tensor rotation matrix. Angles $\boldsymbol{\alpha}^{AM} = \begin{bmatrix} \phi^{AM} & \theta^{AM} & \psi^{AM} \end{bmatrix}^T$ calculated from the measurements of the accelerometers (12, 10, 11) and the magnetometer (17) have a short-duration variation resulting from the noise occurring in the measurement system. As the result, the elements of the matrix $\boldsymbol{R}_{NWU}^{RPY}$ (4) determined from the rotation angles $\boldsymbol{\alpha}^{AM}$ characterize "nervousness". It consists of small and temporary changes in value even if the orientation of the object and the associated IMU system do not change. Also matrix $\boldsymbol{R}_{RPY}^{NWU}$ (3) determined in the process of strapdown integration (42) of the angular velocity $\boldsymbol{\omega}^{G}$ changes slowly due to the error occurring in the measurement system of gyroscopes (18). This change results from a "flow" of the rotation angles calculated on the basis of the obtained angular velocities. As the result, the rotation matrix $\boldsymbol{R}_{RPY}^{NWU}$ conatins unmeasurable values and costitutes the process state in the proposed estimation algorithm. It contains information about the rotation angles of the object relatively to the reference frame. Due to the process model described by equation (44) rotation matrix $\boldsymbol{R}_{RPY}^{NWU}$ is transformed into the state vector in the following way:

$$\boldsymbol{R}_{RPY}^{NWU} = \begin{bmatrix} r_{11} & r_{12} & r_{13} \\ r_{21} & r_{22} & r_{23} \\ r_{31} & r_{32} & r_{33} \end{bmatrix} \Rightarrow \boldsymbol{r} = \begin{bmatrix} r_{11} & r_{12} & r_{13} & r_{21} & r_{22} & r_{23} & r_{31} & r_{32} & r_{33} \end{bmatrix}^T. \tag{47}$$

Using equation (42) the connection between successive rotation coefficients r_{ij} of the vector can be expressed by the equation:

$$\begin{aligned} \boldsymbol{R}_{RPY}^{NWU}(k+1) &= \begin{bmatrix} r_{11,(k+1)} & r_{12,(k+1)} & r_{13,(k+1)} \\ r_{21,(k+1)} & r_{22,(k+1)} & r_{23,(k+1)} \\ r_{31,(k+1)} & r_{32,(k+1)} & r_{33,(k+1)} \end{bmatrix} = \\ &= \begin{bmatrix} r_{11,k} & r_{12,k} & r_{13,k} \\ r_{21,k} & r_{22,k} & r_{23,k} \\ r_{31,k} & r_{32,k} & r_{33,k} \end{bmatrix} \begin{bmatrix} 1 & -\Delta\psi & \Delta\theta \\ \Delta\psi & 1 & -\Delta\phi \\ -\Delta\theta & \Delta\phi & 1 \end{bmatrix} \end{aligned} \tag{48}$$

for $k = 0, 1, 2, \ldots$, where the relationship between the discrete moment of measurement k and the time t is as follows:

$$t = k\Delta t \Rightarrow k = \frac{t}{\Delta t}. \tag{49}$$

Equation (48) defines the relationship between successive (in subsequent measurement times k) coefficients values of rotation matrix:

$$\begin{cases} r_{11,(k+1)} & = r_{11,k} + r_{12,k}\Delta\psi - r_{13,k}\Delta\theta \\ r_{12,(k+1)} & = -r_{11,k}\Delta\psi + r_{12,k} + r_{13,k}\Delta\phi \\ r_{13,(k+1)} & = r_{11,k}\Delta\theta - r_{12,k}\Delta\phi + r_{13,k} \\ r_{21,(k+1)} & = r_{21,k} + r_{22,k}\Delta\psi - r_{23,k}\Delta\theta \\ r_{22,(k+1)} & = -r_{21,k}\Delta\psi + r_{22,k} + r_{23,k}\Delta\phi \\ r_{23,(k+1)} & = r_{21,k}\Delta\theta - r_{22,k}\Delta\phi + r_{23,k} \\ r_{31,(k+1)} & = r_{31,k} + r_{32,k}\Delta\psi - r_{33,k}\Delta\theta \\ r_{32,(k+1)} & = -r_{31,k}\Delta\psi + r_{32,k} + r_{33,k}\Delta\phi \\ r_{33,(k+1)} & = r_{31,k}\Delta\theta - r_{32,k}\Delta\phi + r_{33,k} \end{cases} \tag{50}$$

and formulates the process model for the Kalman filter. Using the relation (50) one can define the following equivalent to the equation (48):

$$\begin{aligned} \boldsymbol{R}_{RPY}^{NWU}(k+1) &= \left(\begin{bmatrix} 1 & \Delta\psi & -\Delta\theta \\ -\Delta\psi & 1 & \Delta\phi \\ \Delta\theta & -\Delta\phi & 1 \end{bmatrix} \begin{bmatrix} r_{11,k} & r_{21,k} & r_{31,k} \\ r_{12,k} & r_{22,k} & r_{32,k} \\ r_{13,k} & r_{23,k} & r_{33,k} \end{bmatrix} \right)^T \\ &= \left(\left(\boldsymbol{I}^{3\times3} + [\boldsymbol{A}\times]\right)^T \left(\boldsymbol{R}_{RPY}^{NWU}(k)\right)^T \right)^T = \left(\left(\boldsymbol{I}^{3\times3} - [\boldsymbol{A}\times]\right) \left(\boldsymbol{R}_{RPY}^{NWU}(k)\right)^T \right)^T . \end{aligned} \tag{51}$$

Considering the above relation and the fact that the angular velocities are obtained at discrete moments of measurement (49) $\boldsymbol{\omega}^G = \boldsymbol{\omega}^G(t) = \boldsymbol{\omega}_k^G$ equation (42) takes the form:

$$\boldsymbol{R}_{RPY,k}^{NWU} = \boldsymbol{R}_{RPY,(k-1)}^{NWU} \boldsymbol{\Omega}_k = \left(\boldsymbol{\Lambda}_k \left(\boldsymbol{R}_{RPY,(k-1)}^{NWU} \right)^T \right)^T \tag{52}$$

where matrix $\boldsymbol{\Lambda}_k$ is expressed by the relation:

$$\boldsymbol{\Lambda}_k = \boldsymbol{\Omega}_k^T = \left(\boldsymbol{I}^{3\times3} + [\boldsymbol{A}\times]_k\right)^T = \boldsymbol{I}^{3\times3} - [\boldsymbol{A}\times]_k = \begin{bmatrix} 1 & \omega_{z,k}\Delta t & -\omega_{y,k}\Delta t \\ -\omega_{z,k}\Delta t & 1 & \omega_{x,k}\Delta t \\ \omega_{y,k}\Delta t & -\omega_{x,k}\Delta t & 1 \end{bmatrix} \tag{53}$$

Equation (52) describes the process in the measurement system IMU. Along with the definition of the state vector $\boldsymbol{x}_k$ as in (47) it finally defines non-stationary linear model of state changes equation for the Kalman filter:

$$\boldsymbol{x}_k = \boldsymbol{F}_k \boldsymbol{x}_{k-1} + \boldsymbol{v}_k \Rightarrow \boldsymbol{r}_k = \begin{bmatrix} \boldsymbol{\Lambda}_k & \boldsymbol{0}^{3\times3} & \boldsymbol{0}^{3\times3} \\ \boldsymbol{0}^{3\times3} & \boldsymbol{\Lambda}_k & \boldsymbol{0}^{3\times3} \\ \boldsymbol{0}^{3\times3} & \boldsymbol{0}^{3\times3} & \boldsymbol{\Lambda}_k \end{bmatrix} \boldsymbol{r}_{k-1} + \boldsymbol{v}_k \tag{54}$$

where the process matrix $\boldsymbol{F}_k$ is time varying and depends on the current value of the angular velocity vector $\boldsymbol{\omega}_k^G$ and $\boldsymbol{0}^{n\times n}$ is the zero matrix of dimension $n\times n$. The output (measured) signal can be defined on the base of the rotation matrix $\boldsymbol{R}_{NWU}^{RPY}$ determined, at the time k, with the rotation angles $\boldsymbol{\alpha}_k^{AM}$ calculated from measurements of accelerometers and magnetometers:

$$\boldsymbol{\alpha}_k^{AM} \Rightarrow \boldsymbol{R}_{NWU,k}^{RPY} \Rightarrow \left(\boldsymbol{R}_{NWU,k}^{RPY}\right)^T \Rightarrow \boldsymbol{r}_k^{AM} = \boldsymbol{y}_k. \tag{55}$$

As the result, the measurement (output) equation model in the Kalman filter takes the form:

$$\boldsymbol{y}_k = \boldsymbol{H}\boldsymbol{x}_k + \boldsymbol{w}_k \Rightarrow \boldsymbol{r}_k^{AM} = \boldsymbol{I}^{9\times 9}\boldsymbol{r}_k + \boldsymbol{w}_k \tag{56}$$

where $\boldsymbol{I}^{n\times n}$ is the identity matrix of dimension $n\times n$.

The results of the Kalman filtering using the model defined by equations (54) and (56) are estimated unmeasurable coefficients of rotation matrix $\boldsymbol{R}_{RPY,k}^{NWU}$. Using the relations (20,21,22,23) and designed in such a way matrix one can find the rotation angles $\boldsymbol{\alpha}_k^* = \begin{bmatrix} \phi_k^* & \theta_k^* & \psi_k^* \end{bmatrix}^T$.

7. Results of experiments

The experiments evaluating the estimation of the rotation angles obtained from the proposed fusion signals algorithm and comparing the results with the reference signal are described below. The evaluation was done using specially designed simulator of the IMU measurement system. The simulator bases on the sensor system which models the accelerometers, magnetometers, and gyroscopes respectively, using equations (6), (13) and (18). The exemplary waveform variation of rotation angles was chosen as follows:

$$\begin{aligned} \phi(t) &= 100\sin(0.45t+2)\ [deg] \\ \theta(t) &= 45\sin(3t+0.8)\ [deg] \\ \psi(t) &= 120\sin(t)\ [deg]. \end{aligned} \tag{57}$$

The equations (57) allow to generate waveforms indicated by the accelerometers, magnetometers and gyroscopes. According to earlier imposed assumptions, simulated object does not introduce additional value of linear acceleration ($\widetilde{\boldsymbol{a}} \approx \boldsymbol{0}$). The values of bias appearing in the model system of gyroscopes in the simulation were set at $0.6\,[deg/s]$:

$$\boldsymbol{\beta} = \begin{bmatrix} 0.6 & 0.6 & 0.6 \end{bmatrix}^T. \tag{58}$$

The measurement noise which appears in the sensor model equations was generated using a random number generator with normal distribution, zero mean value and variances as follows:

$$E\left[\boldsymbol{v}_a\boldsymbol{v}_a^T\right] = 0.5\boldsymbol{I}^{3\times3}$$
$$E\left[\boldsymbol{v}_m\boldsymbol{v}_m^T\right] = 0.01\boldsymbol{I}^{3\times3} \qquad (59)$$
$$E\left[\boldsymbol{v}_\omega\boldsymbol{v}_\omega^T\right] = 0.1\boldsymbol{I}^{3\times3}$$

Fig. 5 shows the waveforms of each rotation angles determined from simulated measurements of accelerometers, magnetometers $\boldsymbol{\alpha}_k^{AM}$ (12,11,17) and gyroscopes $\boldsymbol{\alpha}_k^G$ (24,22,25) for equation (57). The angles $\boldsymbol{\alpha}_k^G$ were determined by the rotation matrix $\boldsymbol{R}_{RPY}^{NWU}$ obtained from strapdown integration (42) of the measurement signal from the gyroscopes. It is also presented the waveforms rotation angles $\boldsymbol{\alpha}_k^*$ determined from the estimated rotation matrix elements using the proposed solution. In order to emphasize effect of measurement noise and bias on the course determined rotation angles of the accelerometer and magnetometer measurements and gyroscopes are presented only towards the first ten and last ten seconds of the simulation.

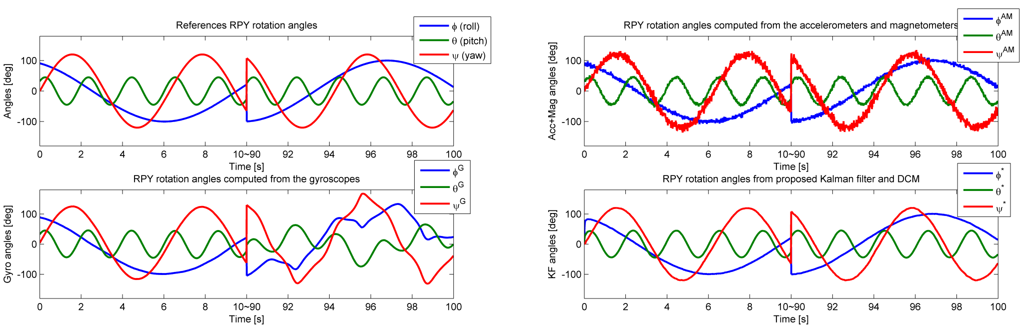

Figure 5. Waveforms of reference and estimated values of the rotation angles (the first and last ten seconds of simulation) - simulation experiment.

In order to assess the quality of the estimation of the rotation angles, vector of the MAE (Mean Absolute Error) is introduced:

$$\mathrm{MAE}\left(\hat{\boldsymbol{\alpha}}\right) = \hat{\boldsymbol{\alpha}}_\varepsilon = \frac{1}{N}\sum_{k=1}^{N}\left|\boldsymbol{\alpha}_k - \hat{\boldsymbol{\alpha}}_k\right| \qquad (60)$$

where $\boldsymbol{\alpha}_k = \begin{bmatrix} \phi_k & \theta_k & \psi_k \end{bmatrix}^T$ is the reference waveform and $\hat{\boldsymbol{\alpha}} \in \left\{\boldsymbol{\alpha}^{AM}, \boldsymbol{\alpha}^G, \boldsymbol{\alpha}^*\right\}$; $\phi - \theta - \psi$ denotes rotation angles determined from: measurements of accelerometers and magnetometers $\boldsymbol{\alpha}_k^{AM} = \begin{bmatrix} \phi_k^{AM} & \theta_k^{AM} & \psi_k^{AM} \end{bmatrix}^T$, gyroscopes $\boldsymbol{\alpha}_k^G = \begin{bmatrix} \phi_k^G & \theta_k^G & \psi_k^G \end{bmatrix}^T$ and the proposed non-stationary Kalman filter algorithm $\boldsymbol{\alpha}_k^* = \begin{bmatrix} \phi_k^* & \theta_k^* & \psi_k^* \end{bmatrix}^T$. Tab. 2 shows MAE values for the presented simulated waveform.

Part of the experiments were devoted to compare the results of estimation of the rotation angles $\boldsymbol{\alpha}_k^{AM}$ designated from accelerometers and magnetometers with the values

Table 2. Mean Absolute Error for references and estimated rotation angles waveforms

MAE $[deg]$	roll (ϕ_ε)	pitch (θ_ε)	yaw (ψ_ε)
$\boldsymbol{\alpha}^{AM}$	2.7871	2.3201	5.6810
$\boldsymbol{\alpha}^{G}$	12.4582	15.6488	17.2366
$\boldsymbol{\alpha}^{*}$	0.6329	0.6845	1.0741

of the angles $\boldsymbol{\alpha}_k^G$ designated from the rotation matrix $\boldsymbol{R}_{RPY}^{NWU}$ which in turn was obtained by using measurements from the gyroscopes and strapdown integration. These results were compared with the values of the angles $\boldsymbol{\alpha}_k^*$ designated from the rotation matrix $\boldsymbol{R}_{RPY}^{NWU}$, represented as a state vector $\hat{\boldsymbol{r}}_k$ (47), which has been calculated from the signals of the IMU sensor.

In the first experiment, successive rotation intervals in the range of about $\pm 90\,[deg]$ was realized with respect only to one axis of the base frame. Respectively: around the X axis (roll angle) in the time interval $T_1 \cong (4 \div 15)\,[s]$, about the Y axis (pitch angle) for $T_2 \cong (19 \div 27)\,[s]$, and around the Z axis (yaw angle) to $T_3 \cong (37 \div 50)\,[s]$. Obtained estimates of the rotation angle values are shown in Fig. 6 (left column).

For comparison, various estimates of the rotation angle show the waveforms of individual angles obtained in three possible ways (Fig. 6 right column).

The aim of the next experiment was to verify behavior of the proposed solution if the orientation of the IMU changes fast. These changes occurred simultaneously with respect to all three axes of the reference frame. The results estimates of $\phi - \theta - \psi$ rotation angles for this test sequence are shown in Fig. 7 (left column). In order to assess the quality of the estimates, they have been compared with the various rotation angles for the time interval $T_4 = (10 \div 18)\,[s]$. Compared angles were obtained from the acceleration, magnetic field and gyroscopes sensor by using the proposed solution (Fig. 7 right column).

8. Conclusion

In this paper, the orientation estimation algorithm based on the non-stationary Kalman filter has been deeply analyzed. The analysis of the example waveforms (e.g first experiment) leads to the conclusion that the angles determined using the proposed solutions have a variation similar to the angles obtained from the accelerometers and magnetometers, but are not fast time-varying what results from the component of noise contained in the IMU measurement systems. As the result, the waveforms are much less "nervous". It can be observed also that the resulting estimate rotation angles do not drift which results from the bias in the measurement system of gyroscopes. By using the Kalman filter in the proposed method, it was possible to eliminate the disadvantages

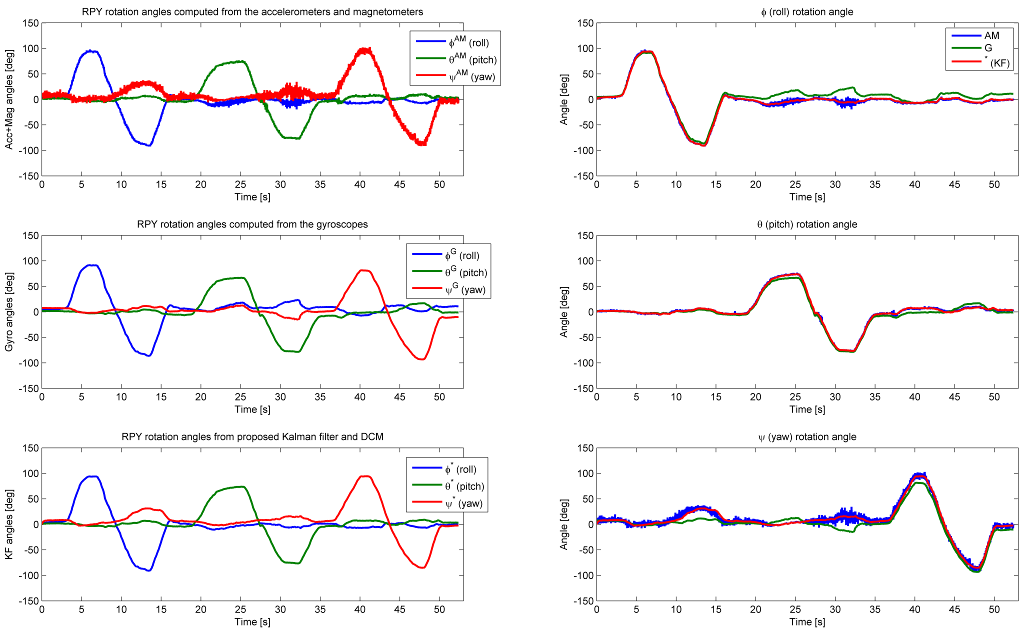

Figure 6. Waveforms designated $\phi - \theta - \psi$ (RPY) rotation angles (left column) and comparison of the individual rotation angles (right column) for the accelerometer and magnetometer (AM), gyroscopes (G) and signals fusion from the IMU - first experiment.

of the solution of the estimate of rotation angle using acceleration, angular velocity and magnetic field sensors.

Analysis of the results of the second experiment confirms the conclusions observed in the first one. It follows then that the proposed solution correctly determines angles of rotation. At the same time, it does not have the drawbacks resulting from the construction of IMU sensor.

The proposed solution allows fast and simple implementation on the platform of the IMU measurement system. The state vector $\boldsymbol{r}_k$ (47) is defined as a nine-element structure. However, due to the nature of the definition of state equation (54) and the properties of the matrix $\boldsymbol{F}_k$ (size 9×9) analyzed solution can be decomposed into three subtasks of a smaller dimensionality. The matrix state equation (54) is a block matrix with submatrix $\boldsymbol{\Lambda}_k$ (53) arranged diagonally. As the result, the state vector $\boldsymbol{r}_k$ can be decomposed into three subvectors $\boldsymbol{r}_k^i$ $i \in \{1,2,3\}$ which define the rows of the rotation matrix $\boldsymbol{R}_{RPY}^{NWU}$:

$$\boldsymbol{R}_{RPY}^{NWU} = \begin{bmatrix} \boldsymbol{r}^1 & \boldsymbol{r}^2 & \boldsymbol{r}^3 \end{bmatrix}^T \Rightarrow \boldsymbol{r}^i = \begin{bmatrix} r_{i1} & r_{i2} & r_{i3} \end{bmatrix}^T \tag{61}$$

for $i = 1,2,3$.

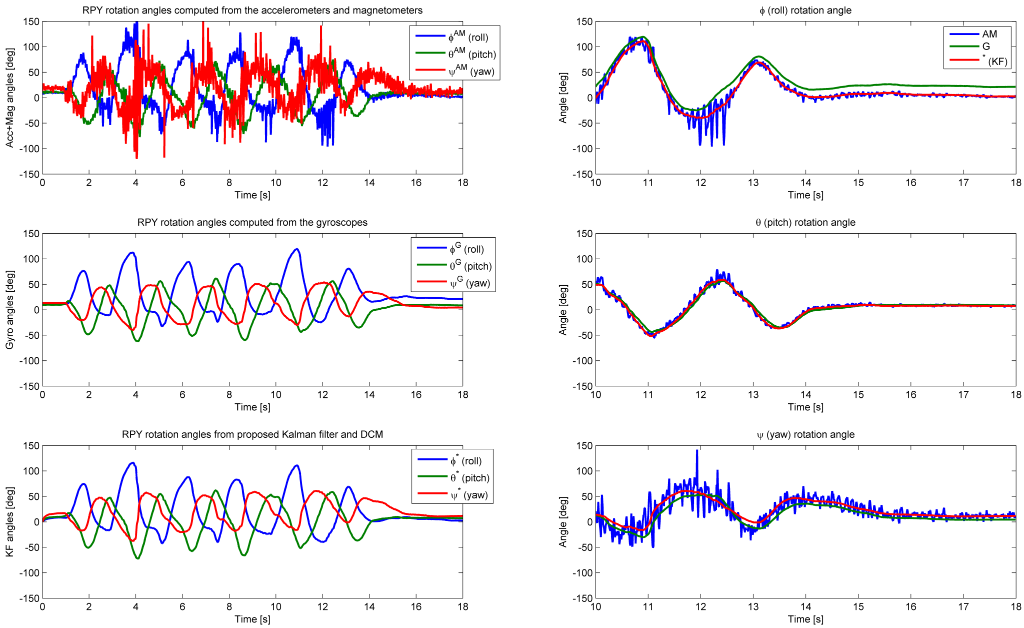

Figure 7. Waveforms designated $\phi-\theta-\psi$ (RPY) rotation angles (left column) and comparison of rotation angles for part of waveforms (right column) for the system (AM), (G) and signals fusion from IMU - second experiment.

Following the above modification, the proposed solution can be decomposed into the three subtasks (simpler Kalman filter) based on the process model as:

$$\begin{aligned} \boldsymbol{x}_k = \boldsymbol{F}_k \boldsymbol{x}_{k-1} + \boldsymbol{v}_k &\Rightarrow \boldsymbol{r}^i_k = \boldsymbol{\Lambda}_k \boldsymbol{r}^i_{k-1} + \boldsymbol{v}^i_k \\ \boldsymbol{y}_k = \boldsymbol{H}\boldsymbol{x}_k + \boldsymbol{w}_k &\Rightarrow \boldsymbol{r}^{i,AM}_k = \boldsymbol{I}^{3\times 3} \boldsymbol{r}^i_k + \boldsymbol{w}^i_k \end{aligned} \tag{62}$$

Each subtask (62) allows the estimation of coefficients of i-th row ($i = 1,2,3$) of the matrix $\boldsymbol{R}^{NWU}_{RPY}$. This decomposition lets a more efficient implementation of the proposed solution on the hardware platform of the IMU measurement system. At the same time it preserves the properties of the result as the proposed solution (54, 56).

References

[1] D. H. Titterton and J. L. Weston: Strapdown Inertial Navigation Technology. The Institution of Electrical Engineers, 2nd ed., 2004.

[2] M. S. Grewal, L. R. Weill and A. P. Andrews: Global Positioning Systems, Inertial Navigation, and Integration. John Wiley & Sons, 2001.

[3] M. GUCMA and J. MONTEWKA: Podstawy morskiej nawigacji inercyjnej. Szczecin: Akademia Morska w Szczecinie, 2006. (in Polish).

[4] S. M. LAVALLE: Planning Algorithms. Cambridge University Press, 2006.

[5] M. EUSTON, P. COOTE, R. MAHONY, J. KIM and T. HAMEL: A complementary filter for attitude estimation of a fixed-wing UAV. In *Proceedings of the IEEE/RSJ Int. Conf. on Intelligent Robots and Systems (IROS)*, (2008), 340-345.

[6] J. KIM: Autonomous Navigation for Airborne Applications. PhD thesis, Australian Centre for Field Robotics, The University of Sydney, 2004.

[7] R. M. MURRAY, Z. LI and S. S. SASTRY: A Mathematical Introduction to Robotic Manipulation. CRC Press, 1994.

[8] D. ROETENBERG: Inertial and Magnetic Sensing of Human Motion. PhD thesis, University of Twente, 2006.

[9] E. R. BACHMANN: Inertial and magnetic tracking of limb segment orientation for inserting humans into synthetic environments. PhD thesis, Naval Postgraduate School Monterey, California, 2000.

[10] D. ROETENBERG, J. HENK, H. J. LUINGE, T. CHRIS, C. T. M. BATEN and P. H. VELTINK. Compensation of magnetic disturbances improves inertial and magnetic sensing of human body segment orientation. *IEEE Trans. Neural Systems and Rehabilitation Engineering*, **13**(3), (2005), 395-405.

[11] J. PUSA: Strapdown inertial navigation system aiding with nonholonomic constraints using indirect Kalman filtering. Master's thesis, Tampere University of Technology, 2009.

[12] S. RÖNNBÄCK: Developement of a ins/gps navigation loop. Master's thesis, Lulea University of Technology, 2000.

[13] P. SADŁOWSKI: Parametryzacje rotacji i algorytmy rozwiązywania równań dynamiki z rotacyjnymi stopniami swobody. PhD thesis, Polskia Akademia Nauk, 2007. (in Polish).

[14] T. HAMEL and R. MAHONY: Attitude estimation on so(3) based on direct inertial measurements. In *Proc. of the IEEE Int. Conf. on Robotics and Automation (ICRA)*, (2006), 2170-2175.

[15] J. F. GUERRERO-CASTELLANOS, H. MADRIGAL-SASTRE, S. DURAND, L. TORRES and G. A. MUNOZ HERNÁNDEZ: A robust nonlinear observer for real-time attitude estimation using low-cost mems inertial sensors. *Sensors*, **13**(11), (2013), 15138-15158.

[16] S. FUX: Development of a planar low cost inertial measurement unit for uavs and mavs. Master's thesis, Eidgenössische Technische Hochschule Zürich, 2008.

[17] K. JASKOT and A. BABIARZ: The inertial measurement unit for detection of position. *Przegląd Elektrotechniczny*, **86**(11a), (2010), 323-333.

[18] M. PEDLEY: Tilt Sensing Using a Three-Axis Accelerometer. Freescale Semiconductor Application Note, rev.5 ed., 2013. n.AN3461.

[19] K. KIM and C. G. PARK: A new initial alignment algorithm for strapdown inertial navigation system using sensor output. In *Proc. of the 17th World Congress. The International Federation of Automatic Control (IFAC)*, (2008), 13034-13039.

[20] T. OZYAGCILAR: Implementing a Tilt-Compensated eCompass using Accelerometer and Magnetometer Sensors. Freescale Semiconductor Application Note, rev.3 ed., 2012. n.AN4248.

[21] O. J. WOODMAN: An Introduction to Inertial Navigation," Tech. Rep. 696, University of Cambridge, 2007.

[22] S. AYUB, A. BAHRAMINISAAB and B. HONARY: A sensor fusion method for smart phone orientation estimation. In *13th Annual Post Graduate Symp. on the Convergence of Telecommunications, Networking and Broadcasting*, (2012).

[23] R. MAHONY, T. HAMEL and J.-M. PFLIMLIN. Non-linear complementary filters on the special orthogonal group. *IEEE Trans. on Automatic Control*, **53**(3), (2008), 1203-1217.

[24] R. GRYGIEL, R. BIEDA and K. WOJCIECHOWSKI: Angles from gyroscope to complementary filter in IMU. *Przegląd Elektrotechniczny*, **90**(9), (2014), 217-224.

[25] E. FOXLIN: Inertial head-tracker sensor fusion by a complementary separate-bias kalman filter. In *Proc. of IEEE Virtual Reality Annual International Symp.*, (1996), 185-194.

[26] X. KONG: Ins algorithm using quaternion model for low cost IMU. *Robotics and Autonomous Systems*, **46**, (2004), 221-246.

[27] L. CONG, E. LI, H. QIN, K. V. LING and R. XUE: A performance improvement method for low-cost land vehicle gps/mems-ins attitude determination. *Sensors*, **15**(3), (2015), 5722-5746.